Rotational Dynamics in Liquid Water: A Simulation Study of Librational Motions

Igor M. Svishchev* and Peter G. Kusalik
Department of Chemistry, Dalhousie University, Halifax, Nova Scotia, Canada B3H 4J3

The rotational dynamics in liquid water have been studied. The power spectra of the single-molecule orientational autocorrelation functions (ACF) have been calculated in molecular dynamics simulations with the SPC/E potential and have been used to characterize various rotational motions of water molecules. Both ordinary and heavy water have been examined at temperatures of −10 and 25 °C. For liquid H_2O at 25 °C the power spectra of the second-order (Raman) orientational ACFs contain three intense bands, centred at *ca.* 500, *ca.* 560 and *ca.* 670 cm^{-1}, and a less intense high-frequency shoulder at *ca.* 820 cm^{-1}. Two intense librational bands with maxima at *ca.* 570 and *ca.* 650 cm^{-1} are present in the power spectrum of the single-dipole orientational ACF for the same system. The average temperature coefficient for the librational frequencies of SPC/E water is found to be about −0.65 cm^{-1} K^{-1}, which agrees well with experimental estimates. A well resolved rototranslational band centred at *ca.* 55 cm^{-1} is observed in the low-frequency region of the power spectra of the single-molecule orientational ACFs. This band is relatively insensitive to temperature variations and shows no isotopic effect.

1. Introduction

The dynamical structure in liquid water is often characterized as a fluctuating network of hydrogen (H-) bonded molecules[1,2] in which specific molecular motions, such as restricted translations and rotations (librations), give rise to a remarkably rich vibrational spectrum in the THz region.[1–22] Many practically important collective phenomena in aqueous media (acoustic[11,17] *etc.*) involve these (low-frequency on a spectroscopic timescale) vibrational motions, and hence they have received a great deal of attention in experimental (Raman and IR)[3–10] and theoretical (computer simulation)[10–16] studies.

The low-frequency Raman studies[1,3,5–8] yield three vibrational bands of librational origin centred at *ca.* 720, *ca.* 550 and *ca.* 450 cm^{-1} and two major translational bands centred at *ca.* 190 and *ca.* 60 cm^{-1}. It is now well documented that the translational band at *ca.* 190 cm^{-1} (usually referred to as an OO stretching mode of water pentamers) shows a pronounced increase in intensity with decreased temperature[3,7] (behaviour which is consistent with an increase in intermolecular H-bonding), while the band at *ca.* 60 cm^{-1} (believed to be induced by OOO bending of three H-bonded molecules) is relatively insensitive to temperature variations.[5,7] In several investigations with supercooled water a weak translational band at *ca.* 260 cm^{-1} has also been reported.[7] The interpretation of this band is that it arises from splitting of the major stretching mode into two components due to the difference in force constants for the vibrational motions parallel and perpendicular to the molecule's dipole axis. In recent studies an additional relaxation mode has been detected[5] which appears as a weak shoulder on the elastic Rayleigh peak with a characteristic Raman frequency of *ca.* 8 cm^{-1} at 25 °C. The structural mechanism responsible for this relaxation process has yet to be clarified; it has been suggested that large rotational motions of water molecules which control the lifetime of H-bonded pentamers give rise to this peak in Raman spectra.[5]

Data from the infrared studies generally support the Raman data in mapping librational and translational modes for liquid water. The major feature of the far-infrared spectrum of water[9,10,18,19,21] is an extremely intense broad band centred at *ca.* 700 cm^{-1} which overlaps at the low-frequency end with a much less intense band with a maximum at *ca.* 200 cm^{-1}. There also exists some evidence for additional contributions at low frequencies to the IR absorption from the 550 and 55 cm^{-1} bands.[9,20,21]

In principle, we can also use computer simulations to study these low-frequency molecular vibrations in liquid water structure and a number of such investigations have been carried out. Impey *et al.*[11] have examined MCY water at several state points. In this work they calculated the power spectra arising from single-particle orientational autocorrelation functions[11,22] and found a single broad librational peak at *ca.* 400–450 cm^{-1}. More recently, extensive simulations with the TIP4P potential[13,14,16] have been carried out. Again, only a single librational mode has been found at a frequency of *ca.* 550 cm^{-1}. However, these results also indicate the presence of a low-lying dumped resonance mode at *ca.* 20 cm^{-1} in the rotational spectra of TIP4P water. It has been suggested in the work of Bertolini and Tani[15] that this mode may be due to rototranslational 'interactions'.

Clearly, many questions still remain concerning both the structure and the physical origin of these low-lying vibrational modes. For example, it remains unclear as to how many librational modes are actually active in a non-polarizable water model. These questions can be most readily addressed through computer simulation. In this paper we present the rotational spectra for the SPC/E model of liquid water in the 10–1000 cm^{-1} region in which the features due to various molecular motions are clearly resolved. These spectra have been obtained *via* Fourier transforms of the single-molecule orientational ACFs. We have also calculated the power spectra of the principal components of the angular velocity ACF. In order to resolve the complex spectral structure in the frequency region under consideration, large storage arrays for these ACFs (thereby providing high-resolution spectra) have been exploited in rather long simulation runs (with production periods of *ca.* 800 ps). In this work two temperatures, −10 and 25 °C, have been examined and both ordinary and heavy water have been studied.

The remainder of this paper is organized as follows. In Section 2 we outline the methodological details of our simulations, and then in Section 3 we present spectra and discuss their origin. Finally, our conclusions are given in Section 4.

2. Simulation Details

In this article we report results from molecular dynamics simulations of liquid water performed with the SPC/E pair-potential.[23] The principal frame is defined in Fig. 1. As in our previous work with SPC/E water,[24] where the spatial distributions of molecules in the local frame were examined, we

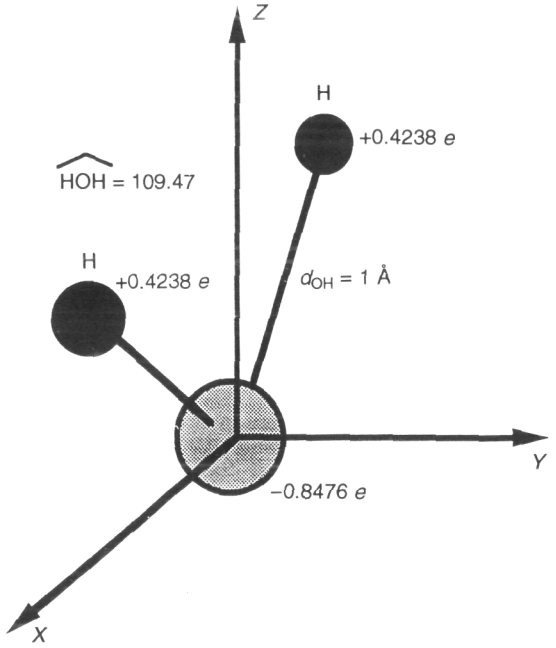

Fig. 1 Principal frame coordinates and geometry of the SPC/E model

have taken the Z-axis to be along the dipole moment and the XZ plane to be the molecular plane. For heavy water the interaction parameters and the corresponding molecular geometry of the SPC/E model were assumed to be unchanged except for the increase of the hydrogen mass.

Our MD simulations have been carried out with samples of 256 molecules at experimental densities at constant temperatures of −10 (H_2O) and 25 °C (H_2O and D_2O). In order to ensure that our spectra did not contain artificial peaks due to the periodic boundaries, test calculations were conducted with 108 particles at 25 °C and no significant changes in the spectral structure were detected. In our calculations isothermal conditions were maintained by means of a Gaussian thermostat.[25] We have utilized a truncated octahedral geometry for the simulation cell[26] and periodic boundary conditions (Ewald sums).[27,28] Our implementation of the Ewald method is described in detail in ref. 24. A fourth-order Gear algorithm[29] with a time step of 1.25 fs was used to integrate the isokinetic equations of motion and the rotational degrees of freedom were represented using quaternions.[27] At each temperature the system was allowed to equilibrate for *ca.* 100 ps and averages were collected over the subsequent 800 ps.

Single-molecule orientational autocorrelation functions have been employed to calculate the spectral functions:

$$I_{k,\alpha}(\omega) = \omega^2 \,\mathrm{Re} \int_0^\infty C_{k,\alpha}(t)\exp(\mathrm{i}\omega t)\,\mathrm{d}t \qquad (1)$$

where

$$C_{k,\alpha}(t) = \langle P_k[\boldsymbol{e}_\alpha(t)\cdot\boldsymbol{e}_\alpha(0)]\rangle \qquad (2)$$

In eqn. (1) and (2), k is a positive integer, $\boldsymbol{e}_\alpha$ ($\alpha = x, y, z$) are the unit vectors of the principal frame, ω is the wavenumber defined as ν/c (ν is the frequency and c is the speed of light), and P_k denotes a Legendre polynomial of order k. The Fourier transforms were carried out after the principal relaxation modes (the long-time exponential decays) have been subtracted from the autocorrelation functions $C_{k,\alpha}(t)$. We remark that the Fourier transforms of the second-order orientational ACFs $C_{2,\alpha}(t)$ can be used to approximate an allowed Raman spectrum for our system, while the transform of the ACF $C_{1,z}(t)$ represents the single-dipole contribution to its allowed IR spectrum.

The statistical errors in our simulated spectra were estimated using the procedure outlined by Allen and Tildesley;[27] they are <0.5%. Large storage arrays, spanning at least two[13] time-steps (*ca.* 10 ps), have been used to accumulate $C_{k,\alpha}(t)$ during simulation runs, since smaller arrays, while requiring less memory, would have resulted in a much lower resolution.

3. Simulation Results and Discussion

Our major simulation results, the Fourier transforms of the single-particle orientational autocorrelation functions of SPC/E water, are presented in Fig. 2 and 3 for ordinary water and Fig. 4 and 5 for heavy water. The transforms of the second-order (Raman) orientational ACFs $C_{2,y}(t)$ and $C_{2,z}(t)$ possess very similar structure (both band shapes and positions of spectral maxima) and hence for reasons of clarity we have plotted only the X and Z contributions. The Fourier transforms of the first-order single-dipole ACF $C_{1,z}(t)$ for ordinary and heavy water are plotted, respectively, in Fig. 3 and 5. To illustrate the temperature dependence in these spectra, data for ordinary water at −10 and 25 °C have been directly compared in Fig. 2 and 3, in which the upper curves are always the low-temperature result. The spectral resolution achieved can be clearly seen in Fig. 2(*b*), 3(*b*), 4(*b*) and 5(*b*), where the discrete points in frequency are explicitly shown.

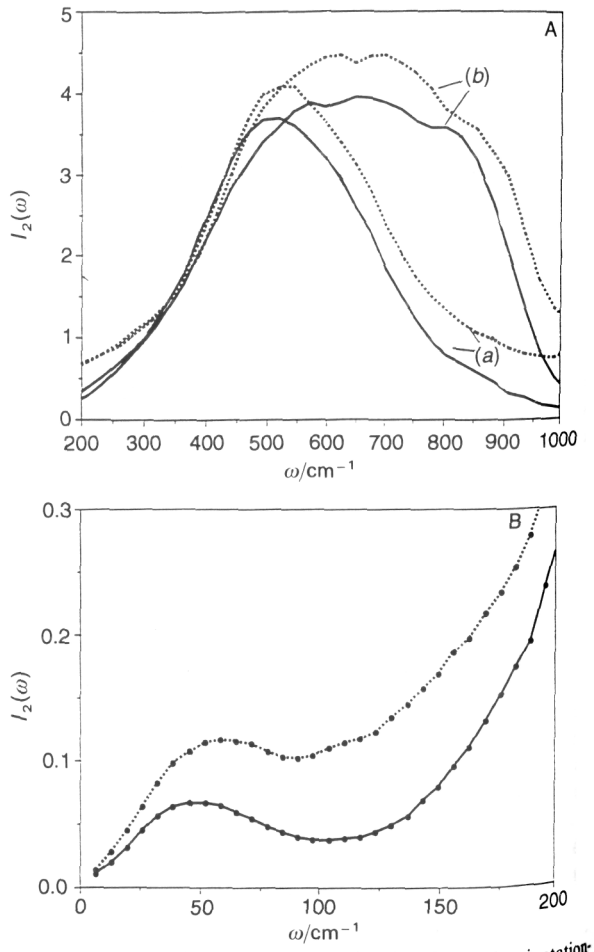

Fig. 2 Fourier transforms of the second-order (Raman) orientational ACFs $C_{2,x}(t)$ (*a*) and $C_{2,z}(t)$ (*b*) for ordinary SPC/E water in the 10–1000 cm^{-1} frequency region. A, High-frequency end; B, low-frequency end. The solid and the dotted lines are, respectively, the results at 25 and −10 °C. In B only $I_{2,x}(\omega)$ is shown.

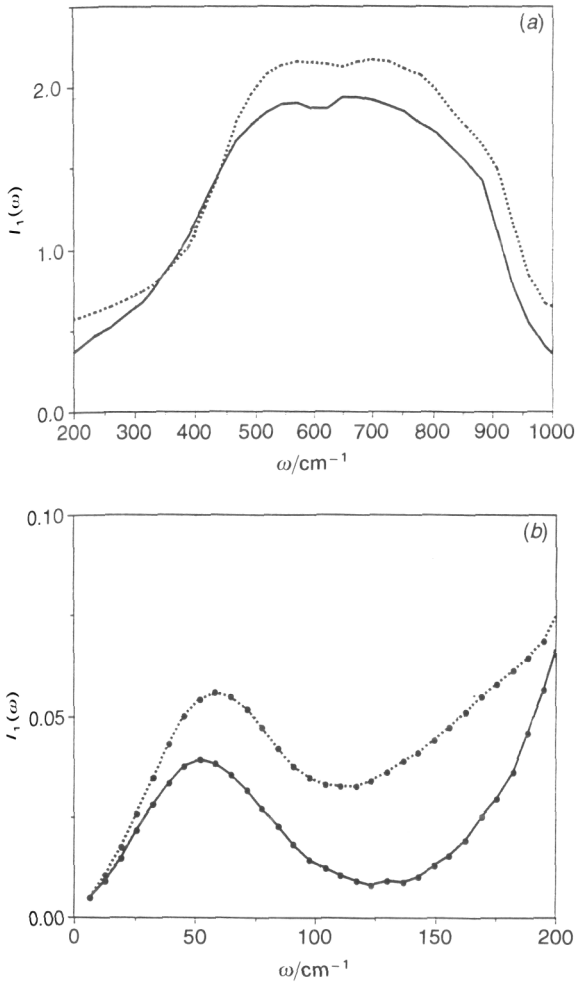

Fig. 3 Fourier transforms of the single-dipole orientational ACF $C_{1,z}(t)$ for ordinary SPC/E water in the 10–1000 cm^{-1} frequency region. (*a*) High-frequency and (*b*) low-frequency end. The solid and the dotted lines are as in Fig. 2.

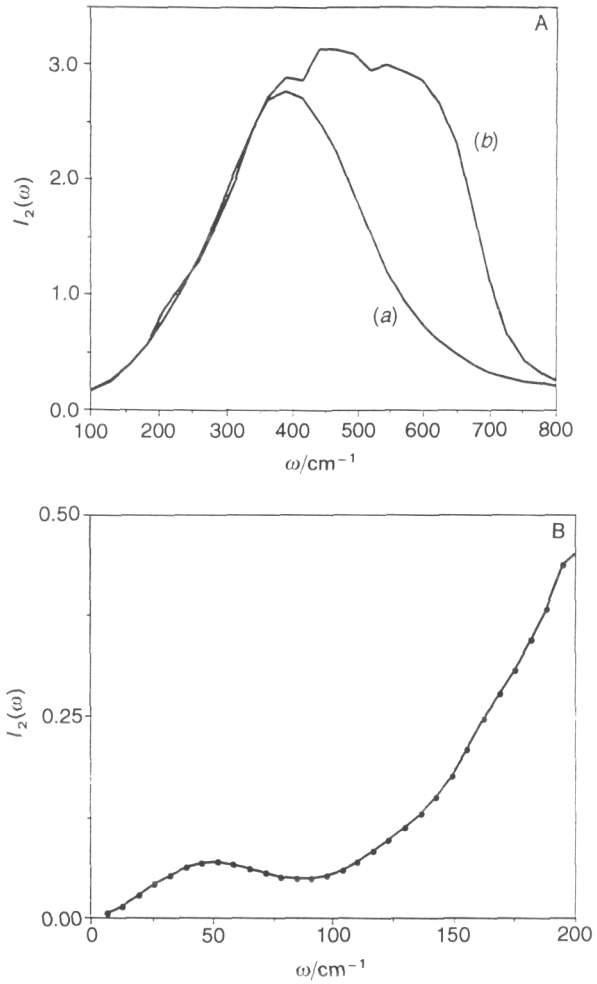

Fig. 4 Fourier transforms of the second-order (Raman) orientational ACFs $C_{2,x}(t)$ (*a*) and $C_{2,z}(t)$ (*b*) for heavy SPC/E water at 25 °C in the 10–1000 cm^{-1} frequency region. A, High-frequency and B, low-frequency end. In B only $I_{2,x}(\omega)$ is shown.

We begin our analysis with the power spectra of the second-order orientational ACFs for liquid H_2O and focus first on the high-frequency end. It can be seen in Fig. 2(*a*) that while the Fourier transform of $C_{2,x}(t)$ has a single librational peak centred at *ca.* 500 cm^{-1} (at 25 °C), the Fourier transform of $C_{2,z}(t)$ has a rather complex structure with major maxima at 560 and 670 cm^{-1}. We point out that all these peaks have been detected, although at slightly different frequencies, in experimental Raman studies.[3,5–7,20] In addition to these major maxima, a high-frequency shoulder at *ca.* 820 cm^{-1} (at 25 °C) is also evident in the spectrum of $C_{2,z}(t)$.

In order to relate these spectral features to specific molecular motions in as direct a way as possible we have also considered the power spectrum of the angular velocity autocorrelation function. In Fig. 6(*a*) the Fourier transforms of the three principal components of the angular velocity ACF are shown (at frequencies 100–1000 cm^{-1}). We observe that the rotational oscillations of water molecules about their *Y* and *Z* axes, as reflected by peaks at 500 cm^{-1} in the power spectra of the *Y* and *Z* components of the angular velocity ACF [see Fig. 6(*a*)], give rise to a nearly symmetric maximum in the $I_{2,x}(\omega)$ [see Fig. 2(*a*)]. At the same time we can see that the more rapid rotations about the *X*-axis essentially do not contribute to the $I_{2,x}(\omega)$. This fact can be explained on the basis of the cumulant expansion of the $C_{k,x}(t)$, in which the leading order dependence does not contain terms due to $\langle\omega_x(t)\omega_x(0)\rangle$.[11] We also find that, unlike molecular rotations about the *Y* and *Z* principal axes, rotational motion about the *X* axis appears more complex; the power spectrum of $\langle\omega_x(t)\omega_x(0)\rangle$ is noticeably skewed toward higher frequencies. This seems to indicate that the fine librational structure in the spectra of the second-order (Raman) orientational ACFs reflects different types of oscillatory motions primarily about the principal *X* axis (given our definition of the local frame).

The librational spectrum of the single-dipole ACF $C_{1,z}(t)$ for liquid H_2O is shown in Fig. 3(*a*) and, as we might expect, its shape appears to be quite similar to that of the second-order ACF $C_{2,z}(t)$. Both major librational peaks, centred at *ca.* 570 and *ca.* 650 cm^{-1}, are present, although the high-frequency peak clearly displayed in $I_{2,z}(\omega)$ is not resolved in $I_{1,z}(\omega)$. We recall that the major difference between experimental IR and Raman spectra at these frequencies arises largely from the fact that only the single-dipole ACF $C_{1,z}(t)$ contributes to the IR spectrum, while the Raman spectrum has contributions from all second-order orientational ACFs.[11,22,30] Correspondingly, the 500 cm^{-1} band which dominates the Raman spectrum is absent in the experimental IR data.

In order to illustrate how temperature affects the librational motions of molecules in SPC/E water, simulation results at −10 and 25 °C have been compared directly in Fig. 2(*a*) and 3(*a*). From these data we have then estimated the average temperature coefficient, $\Delta\langle\omega_{max,\,lib.}(H_2O)\rangle/\Delta T$, for

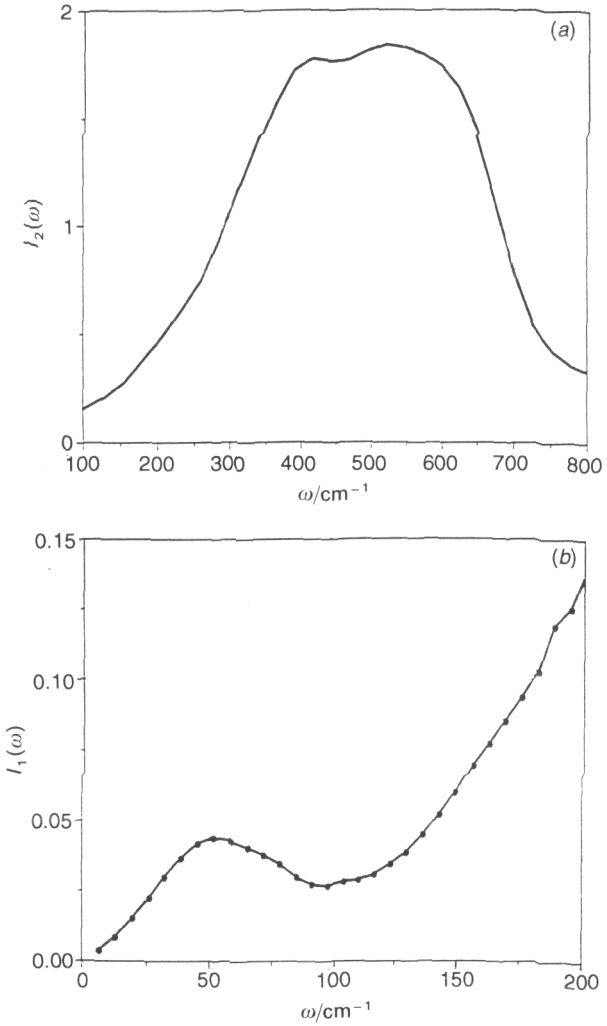

Fig. 5 Fourier transforms of the single-dipole orientational ACF $C_{1,z}(t)$ for heavy SPC/E water at 25 °C in the 10–1000 cm^{-1} frequency region. (*a*) High-frequency and (*b*) low-frequency end.

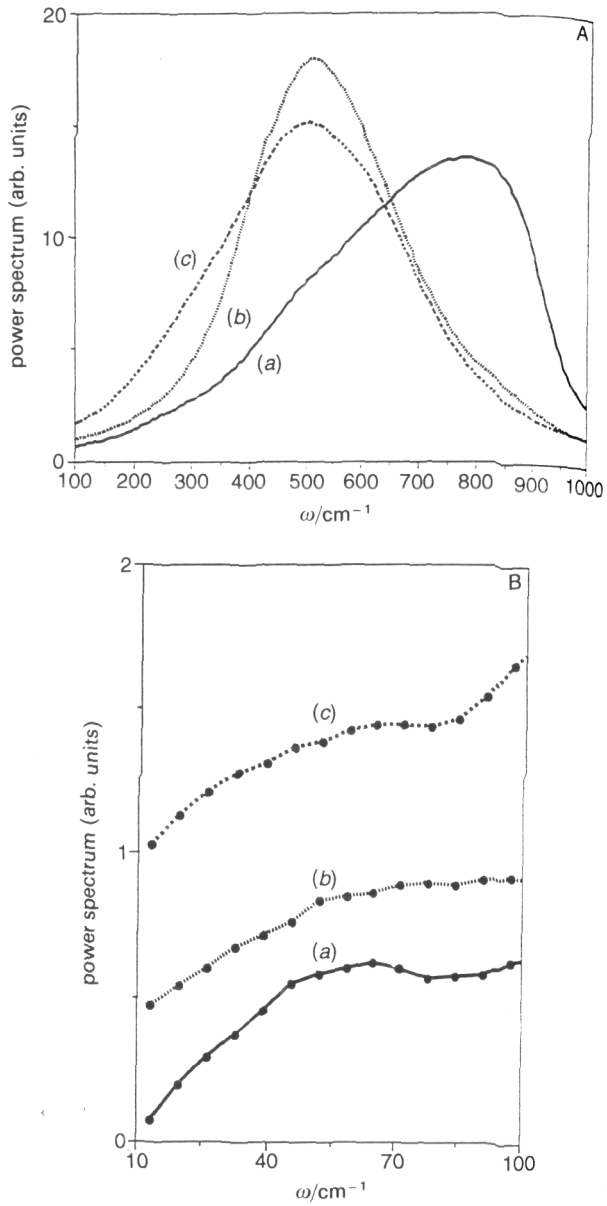

Fig. 6 Power spectra of the angular velocity ACF of ordinary SCF/E water at 25 °C. A, High-frequency and B, low-frequency end. (*a*), (*b*) and (*c*) represent the *X*, *Y* and *Z* principal components, respectively.

the librational frequencies of SPC/E water. The value obtained by averaging over the four observed maxima in $I_{2,x}(\omega)$ and $I_{2,z}(\omega)$ and the two major maxima in $I_{1,z}(\omega)$ is *ca.* -0.65 cm^{-1} K^{-1}. The available experimental estimate from IR data[18] is -0.7 cm^{-1} K^{-1} and we conclude that we have successfully reproduced both the sign and the magnitude of the average temperature coefficient for librational frequencies.

As we might expect, the librational frequencies for SPC/E water exhibit a pronounced isotopic effect. The power spectra of the second-order orientational ACFs for liquid D_2O at 25 °C are given in Fig. 4(*a*) and the corresponding spectrum of the single-dipole ACF is plotted in Fig. 5(*a*). The average isotopic ratio for frequency maxima, $\langle\omega_{max,\,lib.}(D_2O)\rangle/\langle\omega_{max,\,lib.}(H_2O)\rangle$, obtained from the librational peaks in these spectra appears to be *ca.* 1.38, reproducing the ideal isotopic ratio for the water molecule.

We now shift our focus to the low-frequency end (<200 cm^{-1}) in our spectra. As mentioned above, the experimental data indicate the presence of at least two resonance bands in this region centred around 190 and 60 cm^{-1} whose intensity is largely determined by the many-body interaction-induced polarization effects.[12,14–16] Our simulation results in this frequency range from the explicitly non-polarizable SPC/E model are shown in Fig. 2(*b*)–3(*b*) (for H_2O) and Fig. 4(*b*)–5(*b*) (for D_2O). They clearly indicate the presence of a low-lying band centred at *ca.* 55 cm^{-1} (25 °C). It can also be seen that this band is well resolved from the more intense librational peaks. At the same time, we observe that the 190 cm^{-1} band does not appear active in the power spectra of the single-molecule ACFs for SPC/E water.

The low-frequency power spectra of the components of the angular velocity ACF for SPC/E water at 25 °C are shown in Fig. 6(*b*) and it can be seen that they also exhibit shallow maxima at *ca.* 65 cm^{-1}, most evident in the *X* and *Z* components. Given the fact that a peak appears in the power spectrum of the linear-velocity ACF at approximately the same frequency, it becomes apparent that the band at *ca.* 55 cm^{-1} in the spectra of the single-molecule orientational ACFs arises from a coupled rotational–translational motion. This claim is strongly supported by our recent work[31] which explicitly examines rototranslational motion in liquid water.

As we might expect, the rototranslational mode at *ca.* 55 cm^{-1} is rather insensitive to isotopic substitution [compare Fig. 2(*b*) and 4(*b*) or Fig. 3(*b*) and 5(*b*)]. We also find that the temperature coefficient, $\Delta\langle\omega_{max}\rangle/\Delta T$, for this mode is very

small, *ca.* -0.1 cm^{-1} K^{-1}, which agrees with experimental observations.[5]

Another feature of this low-frequency rototranslational band (exhibited in our model spectra at *ca.* 55 cm^{-1}) is that its intensity is rather insensitive to changes in temperature (this becomes clearer after the contribution due to the symmetric librational peak at *ca.* 500 cm^{-1} has been removed from the spectral data in Fig. 2), which is again consistent with experimental observations.[5,7] A remarkable increase in intensity with decreased temperature is well documented in the experimental Raman spectra for another low-lying band,[3b,7] at 190 cm^{-1}, and in early work it was correlated with the degree of association of H_2O molecules in tetrahedrally H-bonded fragments in liquid water structure.[3a] Later, this temperature variation in the experimental Raman spectra was interpreted as a collective interaction-induced polarization effect which accompanies immediate structural changes in real water.[12,13,22] It has also been argued that the 60 cm^{-1} band of the experimental spectra originates from an induced polarization effect.[22] Our results obtained with the non-polarizable SPC/E model, however, indicate that the slow rotational dynamics of individual molecules activates the 55 cm^{-1} mode. This mode, as shown in ref. 12–14, is enhanced in the experimental Raman and IR spectra by many-body polarization contributions. At the same time, the absence of the 190 cm^{-1} band in our simulation data suggests that it is the interaction-induced polarization effect that activates this band in the experimental spectra and governs its temperature behaviour.

Clearly, the simulations with polarizable water models are needed to understand more fully the influence of temperature on the low-frequency region in the optical spectra of liquid water. Sciortino and Corongiu[32] have recently calculated the low-frequency optical spectra for hexagonal ice using the polarizable NCC potential and have compared them with the spectra obtained for the TIP4P model. Their results indicate that the polarizable model is far better at reproducing the positions of experimental bands in the spectra of the ice I_h.

4. Conclusions

In this article we have reported results from MD simulations of liquid water performed with the SPC/E potential. We have analysed the Fourier transforms of the single-molecule orientational autocorrelation functions focussing upon the fine structure of the molecular librational modes. These modes are widely used as probes of the vibrational dynamics in liquid water, yet their previous statistical-mechanical analysis has been limited because of insufficient spectral resolution in simulation data. Both ordinary and heavy SPC/E water have been studied at temperatures of -10 and 25 °C.

Three major librational modes centred at *ca.* 500, *ca.* 560 and *ca.* 670 cm^{-1} and a less intense high-frequency shoulder at *ca.* 820 cm^{-1} have been identified in the spectra of the second-order (Raman) orientational ACFs (liquid H_2O at 25 °C). Two intense librational bands with maxima at *ca.* 570 and *ca.* 650 cm^{-1} have been found in the spectrum of the single-dipole ACF (liquid H_2O and 25 °C). Analysing the principal components of the angular velocity ACF we have clarified that the complex librational structure in these spectra is largely associated with the rotational dynamics of water molecules about the principal X axis. We have also found that the average temperature coefficient for the librational frequencies of SPC/E water agrees well with available experimental estimates.

One of the most interesting features of our simulation data was the presence of a well resolved rototranslational mode centred at *ca.* 55 cm^{-1} which is relatively insensitive to temperature variations. This mode has been well characterized in experimental Raman studies. We have also found that another characteristic low-lying mode, active in experimental spectra at *ca.* 190 cm^{-1}, is absent in the spectra of the single-molecule orientational ACFs for SPC/E water. This observation supports the claim that its origin in experimental optical spectra is due to interaction-induced polarization effects accompanying structural transformations in liquid water.

We are grateful for the financial support of the Natural Sciences and Engineering Research Council of Canada.

References

1 G. E. Walrafen, in *Water—A Comprehensive Treatise*, ed. F. Franks, Plenum Press, New York, 1972, vol. 1.
2 M. G. Sceats, M. Stavola and S. A. Rice, *J. Chem. Phys.*, 1979, **70**, 3927.
3 (*a*) G. E. Walrafen, *J. Chem. Phys.*, 1964, **40**, 3249; (*b*) G. E. Walrafen, M. R. Fisher, M. S. Hokmabadi and W-H. Yang, *J. Chem. Phys.*, 1986, **85**, 6970.
4 D. Eisenberg and W. Kauzmann, *The Structure and Properties of Water*, Oxford University Press, Oxford, 1969.
5 K. Mizoguchi, Y. Hori and Y. Tominaga, *J. Chem. Phys.*, 1992, **97**, 1961.
6 Y. Yeh, J. H. Bilgram and W. Kanzig, *J. Chem. Phys.*, 1982, **77**, 2317.
7 S. Krishnamurthy, R. Bansil and J. Wiafe-Akenten, *J. Chem. Phys.*, 1983, **79**, 5862.
8 V. Mazzacurati, A. Nucara, M. A. Ricci, R. Ruocco and G. Signorelli, *J. Chem. Phys.*, 1990, **93**, 7767.
9 O. A. Simpson, B. L. Bean and S. Perkowitz, *J. Opt. Soc. Am.*, 1979, **69**, 1723.
10 P. Schiebener, J. Straub, J. M. H. Levelt Sengers and J. S. Gallagher, *J. Phys. Chem. Ref. Data*, 1990, **19**, 677.
11 R. W. Impey, P. A. Madden and I. R. McDonald, *Mol. Phys.*, 1982, **46**, 513.
12 P. A. Madden and R. W. Impey, *Chem. Phys. Lett.*, 1986, **123**, 502.
13 R. Frattini, M. Sampoli, M. A. Ricci and G. Ruocco, *Chem. Phys. Lett.*, 1987, **141**, 297.
14 M. A. Ricci, G. Ruocco and M. Sampoli, *Mol. Phys.*, 1989, **67**, 19.
15 D. Bertolini and A. Tani, *Mol. Phys.*, 1992, **75**, 1065.
16 V. Mazzacurati, M. A. Ricci, G. Ruocco and M. Sampoli, *Chem. Phys. Lett.*, 1989, **159**, 383.
17 S. Sastry, F. Sciortino and H. E. Stanley, *J. Chem. Phys.*, 1991, **95**, 7775.
18 D. A. Draegert, N. W. B. Stone, B. Curnutte and D. Williams, *J. Opt. Soc. Am.*, 1966, **56**, 64.
19 C. W. Robertson, B. Curnutte and D. Williams, *Mol. Phys.*, 1972, **20**, 183.
20 J. B. Hasted, *Aqueous Dielectrics*, Chapman and Hall, London, 1973.
21 J. B. Hasted, S. K. Husain and F. A. M. Frescura and J. R. Birch, *Chem. Phys. Lett.*, 1985, **159**, 622.
22 P. A. Madden, in *The Physics and Chemistry of Aqueous Ionic Solutions*, ed. M-C. Belissinet and G. W. Neilson, Reidel, Dordrecht, 1987, p. 181.
23 H. J C. Berendsen, J. R. Grigera and T. P. Straatsma, *J. Phys. Chem.*, 1987, **91**, 6269.
24 I. M. Svishchev and P. G. Kusalik, *J. Chem. Phys.*, 1993, **99**, 3049.
25 D. J. Evans and J. P. Morriss, *Statistical Mechanics of Nonequilibrium Liquids*, Academic Press, San Diego, 1990.
26 D. Fincham and D. M. Heyes, *Adv. Chem. Phys.*, 1985, **63**, 493.
27 M. P. Allen and D. J. Tildesley, *Computer Simulations of Liquids*, Oxford University Press, Oxford, 1987.
28 P. G. Kusalik, *J. Chem. Phys.*, 1990, **93**, 3520.
29 D. J. Evans and J. P. Morriss, *Comput. Phys. Rep.*, 1984, **1**, 297.
30 P. A. Madden, in *Liquids, Freezing and Glass Transition*, ed. J. P. Hansen, D. Levesque and J. Jinn-Justin, North Holland, Amsterdam, 1991, p. 549.
31 I. M. Svishchev and P. G. Kusalik, *Chem. Phys. Lett.*, 1993, **215**, 596.
32 F. Sciortino and G. Corongiu, *Mol. Phys.*, 1993, **79**, 547.

Paper 3/07030C; *Received* 10*th December*, 1993